This is a repository copy of *Detection and characterization of mosaicism in autosomal dominant polycystic kidney disease*.

White Rose Research Online URL for this paper:
https://eprints.whiterose.ac.uk/205713/

Version: Accepted Version

Article:
Hopp, K. orcid.org/0000-0002-2420-2358, Cornec-Le Gall, E., Senum, S.R. orcid.org/0000-0002-5489-9117 et al. (17 more authors) (2020) Detection and characterization of mosaicism in autosomal dominant polycystic kidney disease. Kidney International, 97 (2). pp. 370-382. ISSN 0085-2538

https://doi.org/10.1016/j.kint.2019.08.038

Article available under the terms of the CC-BY-NC-ND licence (https://creativecommons.org/licenses/by-nc-nd/4.0/).

Reuse
This article is distributed under the terms of the Creative Commons Attribution-NonCommercial-NoDerivs (CC BY-NC-ND) licence. This licence only allows you to download this work and share it with others as long as you credit the authors, but you can't change the article in any way or use it commercially. More information and the full terms of the licence here: https://creativecommons.org/licenses/

Takedown
If you consider content in White Rose Research Online to be in breach of UK law, please notify us by emailing eprints@whiterose.ac.uk including the URL of the record and the reason for the withdrawal request.

eprints@whiterose.ac.uk
https://eprints.whiterose.ac.uk/

Detection and Characterization of Mosaicism in Autosomal Dominant Polycystic Kidney Disease (ADPKD)

Katharina Hopp, Ph.D.[1,2], Emilie Cornec-Le Gall, M.D., Ph.D.[2,5,6], Sarah R. Senum[2], Iris BAW. te Paske, M.Sc.[2], Sonam Raj, Ph.D.[2], Sravanthi Lavu, M.B.B.S.[2], Saurabh Baheti M.S.[3], Marie E Edwards[2], Charles D Madsen, C.C.R.P[2], Christina M Heyer[2], Albert CM Ong, D. M.[7], Kyongtae T. Bae, M.D., Ph.D.[8], Richard Fatica, M.D.[9], Theodore I. Steinman, M.D.[10], Arlene B Chapman, M.D.[11,12], Berenice Gitomer, Ph.D.[1], Ronald D Perrone, M.D.[13], Frederic F Rahbari-Oskoui, M.D.[12], Vicente E Torres, M.D., Ph.D.[2], the HALT Progression of Polycystic Kidney Disease Group, the ADPKD Modifier Study, and Peter C Harris, Ph.D.[2,4]

[1]Division of Renal Diseases and Hypertension, University of Colorado Denver Anschutz Medical Campus, Aurora, CO, USA; [2]Division of Nephrology and Hypertension, [3]Division of Biomedical Statistics and Informatics, and [4]Department of Biochemistry and Molecular Biology, Mayo Clinic, Rochester, MN, USA; [5]Department of Nephrology, Centre Hospitalier Universitaire de Brest, Université de Brest, Brest, France, [6]National Institute of Health and Medical Sciences, INSERM U1078, Brest, France; [7]Kidney Genetics Group, Academic Nephrology Unit, University of Sheffield, Sheffield, UK; [8]Department of Radiology, University of Pittsburgh School of Medicine, Pittsburgh, PA, USA, [9]Department of Nephrology and Hypertension, Cleveland Clinic, Cleveland, OH, USA, [10]Renal Division, Beth Israel Deaconess Medical Center, Boston, MA, USA, [11]Division of Nephrology, University of Chicago School of Medicine, Chicago, IL, USA; [12]Department of Internal Medicine, Emory University School of Medicine, Atlanta, GA, USA, [13]Division of Nephrology, Tufts University Medical Center, Boston, MA, USA

Running Head: ADPKD Mosaicism

Corresponding author: Peter C. Harris, Division of Nephrology and Hypertension, Mayo Clinic, Stabile 7, 200 First Street SW, Rochester, MN 55905. Email: harris.peter@mayo.edu

Word Count = 3982
Abstract = 239

Abstract

Autosomal dominant polycystic kidney disease (ADPKD) is an inherited, progressive nephropathy accounting for 4-10% of end stage renal disease worldwide. *PKD1* and *PKD2* are the most common disease loci, but even accounting for other genetic causes, ~7% of families remain unresolved. Typically, these unsolved cases have relatively mild kidney disease and often have a negative family history. Mosaicism, due to *de novo* mutation in the early embryo, has rarely been identified by conventional genetic analysis of ADPKD families. Here we screened for mosaicism by employing two next generation sequencing (NGS) screens, specific analysis of *PKD1* and *PKD2* employing long-range PCR, or targeted capture of cystogenes. We characterized mosaicism in 20 ADPKD families; the mutation was transmitted to the next generation in five families and sporadic in 15. The mosaic mutation was newly discovered by the NGS in 13 families, and these methods precisely quantified the level of mosaicism in all. All of the mosaic cases had *PKD1* mutations, 14 were deletions or insertions, and 16 occurred in females. Analysis of kidney size and function showed the mosaic cases had milder disease than a control *PKD1* population, but only a few had clearly asymmetric disease. These results show that in a typical ADPKD population, readily detectable mosaicism by NGS accounts for ~1% of cases, and ~10% of genetically unresolved cases with an uncertain family history. Identification of mosaicism is important to fully characterize ADPKD populations and provides informed prognostic information.

Keywords

ADPKD, PKD1, Mosaicism, Genotype/Phenotype Correlations, Mutations, Diagnostics, Prognostics

Introduction

Tuberous sclerosis (TSC) is an example of a dominant disease where *de novo* mutations are common, accounting for 60-70% of cases[1]. These new mutations usually happen in germ cells but can occur postzygotically, resulting in mosaicism where the subject is composed of cells with and without the mutation. Mosaic mutations can be difficult to detect by Sanger sequencing (SS), and when targeted capture next generation sequencing (tNGS) was applied to the 10-15% of TSC patents with no (Sanger) mutation identified (NMI), 49% were found to be mosaics[2]. Hence, mosaicism is a diagnostic challenge but its identification is important to fully characterize a population for family planning purposes, and to determine likely disease severity within a family.

Population studies indicate that 10-20% of autosomal dominant polycystic kidney disease (ADPKD) families can be traced to a *de novo* mutation within living generations[3, 4]. ADPKD is a late-onset, systemic, inherited disorder with a worldwide prevalence of ~1 in 1000[5]. It is characterized by the development and growth of kidney cysts, resulting in end stage renal disease (ESRD) in ~50% of individuals by 60y[6]. The major ADPKD genes are *PKD1* (~78% of pedigrees) and *PKD2* (~15%); PKD1 is associated with more severe disease, and *PKD1* truncating (*PKD1*^{T}) alleles are more severe than nontruncating (*PKD1*^{NT})[7-9]. A small proportion of NMI cases have mutations to other genes, e.g. *GANAB*, *DNAJB11,* or *HNF1B,* but ~7% remain unresolved[10-13]. Mutation screening of *PKD1* is complicated by the presence of six pseudogenes, traditionally requiring a long-range PCR (LR-PCR) approach for SS[14]. More recently, LR-NGS and specifically designed tNGS approaches have been shown to successfully screen this locus[15, 16, 17, 18].

Mosaicism is a possible explanation for NMI cases since they often have a negative/indeterminate family history, typically milder disease, and sometimes an asymmetric/unilateral renal disease presentation; five mosaic ADPKD families have been described[4, 9, 19]. One with gonadal and somatic mosaicism (mixed) illustrated the complexity of identifying a potential living related donor by linkage analysis alone[20]. In a second, an affected father with two ADPKD daughters had the familial large deletion in just ~15% of cells[21]. Other examples showed milder than expected disease for a *PKD1*^{T} mutation in a mosaic mother[22], LR-NGS analysis detected low level mosaicism (3-10%) in different cell types[23], and quantitative PCR and cloning detected mosaicism in a patient

with asymmetric disease[4]. Importantly, all described cases were identified because an offspring had fully penetrant disease.

Here, we employed two NGS approaches to detect and characterize mosaicism in 20 ADPKD pedigrees.

Results

Next generation sequencing analysis to detect mosaicism

To detect mosaicism, two NGS methods were employed, a modified LR-NGS screen of just *PKD1* and *PKD2*[15] and a tNGS panel of 65 or 137 cystogenes (Table S1)[12]. The LR-NGS screen included 110 ADPKD patients with a known/suspected negative family history and NMI from SS of *PKD1* and *PKD2*. Five suspected mosaics detected by family/conventional analysis were controls. The tNGS screening included 723 SS *PKD1*/*PKD2* NMI subjects[12] and 497 unscreened ADPKD subjects. Previous analysis showed good coverage of the duplicated *PKD1* gene using this tNGS approach[12]. Both screening methods have the advantage over whole exome sequencing (WES) of high average sequence read depth (LR-NGS *PKD1*=7317, *PKD2*=10988; 65-Gene-tNGS *PKD1*=839; *PKD2*=475; 137-Gene-tNGS *PKD1*=619; *PKD2*=779; Table S2), allowing detection of pathogenic variants found in just a small percentage of reads.

Two families illustrated the need for caution in defining mosaic cases and the value of employing NGS plus Sanger methodologies. In pedigree M796, SS of individual II-2 suggested a missense mutation at a low level but subsequent tNGS analysis showed that 581/1130 reads (51%) had the pathogenic variant (Figure S1A-C). Follow up SS consistently showed low level signal of the mutation (Figure S1B). These SS findings are likely explained by allele dropout due to a polymorphism under the LR or exon specific PCR primer. Family P1317 showed the opposite scenario where tNGS identified a 26 bp duplication in just 7.9% of reads in II-1 (Figure S1D,E). However, SS showed the duplication to be equally represented (Figure S1F), and subsequently the patient was found to have a positive family history; highlighting, that using tNGS, larger duplications may be captured inefficiently

Definitions and details of the detected mosaic cases

To be certain that the described cases are genuine mosaics, we required the pathogenic variant to be consistently detected at a reduced level by NGS and SS or also

detected by allele specific-PCR (AS-PCR). To avoid calling cases with apparent small reductions in read representation that may be false mosaics, the mutant allele needed to be present in 1-25% of reads (2-50% of the expected level); two exceptions (Pedigrees 390010 and 790057) are explained below. Table 1 describes the detected mosaic mutations to *PKD1* and clinical information of the 20 resolved families. All families have a negative or equivocal family history, with details and diagnostic information summarized in Table 2.

Families with a transmitted *PKD1* mosaic variant (mixed)

In five families, the mosaicism was somatic but the pathogenic variant was also germinal, since the mutation was transmitted to the next generation. Mosaicism was suspected from SS of Family 590013 since the frameshifting change detected in the son (III-1) was only apparent at a low level in the affected mother (II-2; Figure 1A,B). tNGS analysis confirmed the mutant allele in just 157/906 reads (17.3%) compared to 702/1415 (49.6%) in III-1 (Figure 1C). Asymmetric disease was seen in II-2, with a few large cysts in the left kidney, in contrast to multiple small cysts detected in III-1 (Figure 1D,E). II-2 had normal renal function at 56y.

In Family 690020, a *PKD1*^{T} mutation was readily detected by SS in III-1, but only found in the mother (II-2) after focused analysis (Figure 1F,G). LR-NGS identified the change in II-2 in 589/6476 reads (9.1%). II-2's ultrasound (US) imaging showed moderately enlarged kidneys at 61y, while III-1 had significantly enlarged kidneys (Mayo Imaging Class; MIC-1C[8]; Figure S2A); II-2 has just mild renal impairment at 67y.

Individual 870348 II-2 was initially screened by tNGS and found to have a deletion in 515/6247 reads (8.2%; Figure 1H). The deletion was confirmed at a low level by SS and AS-PCR (Figures 1I, S2B). II-2 has multiple bilateral cysts (MIC-1B), with normal renal function at 47y (Figure 1J). One son, III-1, was diagnosed at 26y.

Initial SS of 590046 II-4 did not identify a likely mutation; however, SS of the son (III-2) detected a single codon deletion. LR-NGS of II-2 showed that 899/12858 reads (7.0%) had the deletion, which was confirmed by close inspection of the Sanger sequence (Figure 1K,L). II-4 had an atypical radiological presentation (MIC-2A) with one large kidney and liver cyst and normal renal function at 56y (Figure 1M). Two sons were affected, and mild cystic disease (MIC-1B) was characterized in III-2 at 19y (Figure 1N).

SS of 390010 III-1 identified a large inframe deletion, but it was not detected in his affected mother (II-2) (Figure 1O). LR-NGS also did not readily detect the variant in II-2 but careful analysis showed that 6/4246 reads (0.1%) contained the deletion. SS of AS-PCR showed the deleted sequence in III-1 and a mixture of the normal and deleted sequence in II-2, reflecting an enrichment of the rare deleted sequence (Figure 1P). Imaging of II-2 at 48y showed very mild cystic disease (MIC-1A) and normal renal function at 52y, while the disease in III-1 was more typical for an *PKD1*^{T} mutation (MIC-1D; Figure 1Q,R).

Families with a mosaic variant in a single individual (somatic)

Fifteen families had a somatic mosaic *PKD1* mutation that was not shown to be transmitted. 790057 II-2 was suspected of a whole exon deletion from multiplex ligation-dependent probe amplification (MLPA), but the level of signal suggested mosaicism (Figure 2A,B). Reanalysis by LR-NGS confirmed the deletion and SS of a breakpoint fragment defined it (Figures 2C, S2C). Analysis of read depth within (4731) and flanking the deletion (7810) indicated that 37.7% reads had the deletion; a margin, along with the MLPA data, consistent with mosaicism. The disease of II-2 was moderately severe (MIC-1C; Figure 2D), but with normal renal function at 31y.

In 590039 II-4, MLPA detected an apparently mosaic multiexon deletion (Figure 2E,F). The deletion was not found by the LR-NGS assay since it spanned the end of a LR-PCR product (Table S3), but the deletion was detected by tNGS 49/167 reads (22.7%) from blood derived DNA; 25.5% in PLD tissue (Figure S2D). Analysis of breakpoint reads and amplifying across the deletion defined the mutation (Figure 2G, S2E). The PKD in II-4 was severe (MIC-1D), resulting in ESRD at 55y, and she also had severe PLD that required partial liver resection (Figure 2H).

M484 II-8 was negative from SS but a single nucleotide duplication was detected by both LR-NGS, 1152/5207 reads (20.6%) and tNGS, 518/2578 reads (20.1%), and confirmed by re-SS (Figure 2I,J). II-8 had quite severe kidney disease (MIC-1C), but normal renal function at 47y, and severe PLD requiring cyst aspiration (Figure 2K).

A possible mosaic frameshifting deletion was detected by SS in M375 II-3 that was confirmed and quantified in 930/4858 reads (19.1%) by LR-NGS (Figure 2L,M). The ADPKD was mild (MIC-1B) with normal renal function at 34y (Figure 2N).

290001 II-1 was negative from SS but a nonsense mutation was detected by the LR-NGS in 1296/7347 reads (17.5%) and tNGS in 1045/5061 reads (20.6%), and seen at a low level after re-SS (Figure 2O,P). US identified multiple bilateral cysts and the patient had Stage 3b CKD at 66y.

Initial SS of 870005 II-2 was negative, but tNGS identified a frameshifting mutation in 84/566 reads (14.8%), which was subsequently seen at a low level in the SS by visual inspection (Figure 3A,B). This patient had moderately severe PKD (MIC-1C), moderate PLD, but normal renal function at 54y (Figure 3C).

SS was negative in M646 II-3 but tNGS identified the missense variant p.Pro2809Leu in 454/3392 reads (13.4%), that was subsequently seen at a low level by SS (Figure 3D,E). p.Pro2809Leu is a non-conservative substitution of a residue invariant in orthologs to fish, is not listed in gnomAD[24], and has been described as a likely pathogenic variant[14]. II-3 has relatively small, asymmetric kidneys (MIC-1B; Figure 3F) and has Stage 3b CKD at 60y.

870452 II-1 was only screened by tNGS that detected a typical splicing change in 162/1208 reads **(**13.4%), that was confirmed by SS (Figure 3G,H). The patient had normal renal function at 57y.

M1312 II-2 was screened initially by tNGS that revealed a frameshifting insertion in 199/1637 reads (12.2%). This insertion was not detected by SS but AS-PCR amplified only from the patient's DNA, and SS confirmed the insertion in the AS-PCR product (Figure 3I,J, S2F). Imaging showed multiple kidney cysts, including a large one, but renal function was normal at 36y (Figure 3K).

SS of 290034 II-3 was negative but analysis by both LR-NGS, 786/6407 reads (12.3%) and tNGS, 523/4352 reads (12.0%), detected a mosaic frameshifting deletion that was subsequently confirmed by close examination of the SS (Figure 3L,M). II-3 has moderate kidney disease (MIC-1C and Stage 3b CKD at 68y).

In patient M1327 II-2, no mutation was detected by clinical SS but tNGS detected a frameshifting deletion in 134/1489 reads (9.0%), that was confirmed by repeat SS; the parents were negative for the mutation (Figure 4A,B). II-2 had relatively mild PKD, MIC-1B, and normal renal function at 48y (Figure 4C).

A mutation was suspected but undefined by SS in M855 II-4 and then characterized by LR-NGS as a deletion/insertion mutation in 725/8889 reads (8.2%; Figure 4D,E). The kidney phenotype was mild cystic disease (MIC-1B) with normal renal function at 47y (Figure 4F).

No mutation was detected in 290084 II-7 by initial SS but a conservative missense change (p.Glu574Asp) was found by both LR-NGS, 423/7044 reads (6.0%) and tNGS, 279/3540 reads (7.3%), and confirmed by AS-PCR (Figure 4G,H, S2G). The substitution, c.1722G>T, changes the last nucleotide of exon 8 and is predicted to result in loss of the IVS8 donor site (Figure S2G legend). The patient has normal renal function at 53y but relatively large kidneys (MIC-1C) and severe PLD (Figure 4I).

Initial SS of M174 II-1 was negative but a nonsense mutation was detected by LR-NGS, 427/6018 reads (7.1%) and tNGS, 40/1159 reads (3.5%), and confirmed by AS-PCR and SS (Figure 4J,K, S2H). The patient has rather few, larger cysts in each kidney and reached ESRD at 83y (Figure 4L).

290114 II1 was mutation negative from initial SS but the LR-NGS, 304/7506 reads (4.1%) and tNGS, 46/3490 reads (1.3%), identified a deletion extending over a splice junction. This was subsequently confirmed by re-SS (Figure 4M,N). This patient has relatively mild cystic disease (MIC-1B) and normal renal function at 40y (Figure 4O).

Phenotypic features of the mosaic individuals

We compared the eGFR and height adjusted total kidney volume (htTKV) for the mosaic cases to a non-mosaic Mayo PKD1 population with similar mutation types; truncating or strongly predicted nontruncating mutations (Mutation Strength Group [MSG]1 and 2)[9]. This analysis showed the mosaic group had a greater eGFR of 30.2 mL/min/1.73 m^2 ($p<0.001$) and a htTKV 32.5% ($p=0.021$) smaller than the controls, but there was little correlation between the level of the mosaic mutant allele and either phenotype (Figure 5A,B).

Discussion

We describe here two NGS methods to robustly detect mosaic mutations (~2-50% expected allele level) in the *PKD1* or *PKD2* gene, including in the duplicated region of *PKD1*. Unlike previous descriptions of ADPKD mosaicism, 15 mutations were detected when just one family member was affected. Where both methods were employed (6 cases), there was good agreement in the mutant allele level, which is more quantifiable and reliable than from SS. Both methods have good read depth over most parts of the screened genes, although read depth was lower for both in very GC-rich regions (Table S2), but the much easier application of tNGS versus LR-PCR means it is likely to be more widely employed[15, 17, 18]. The greater read depth, plus better coverage of *PKD1,* shows the value of a targeted approaches for screening (especially for mosaicism) of this gene compared to WES[17, 18, 25]. Here we did not attempt to identify patients with possible high-level mosaicism (50-90% expected level), since further study is needed to reliably differentiate mosaicism from *de novo* germline mutations.

Detecting mosaicism is important as it can genetically resolve SS NMI cases (13 families in this study). Also, it provides important prognostic information; on average the kidney disease in mosaics is milder than expected for the mutation type, although the level of mosaicism in blood cell DNA did not strongly correlate with disease severity. This presumably reflects that the level of the mutant allele in the kidney that can diverge considerably from that in blood cells. Interestingly, three mosaics had severe PLD, consistent with previous data that ADPKD genotype is less important for the development of liver versus kidney disease[26]. In the one case where severe PLD tissue was assayed, the level of the mutant allele was only slightly higher than in the blood cell DNA.

In transmitted cases, knowledge that the disease is likely to be more severe in the offspring is important. In the families studied here, the mutant allele was transmitted in 25% of cases. There is likely a positive bias in detecting cases with a fully penetrant offspring, but many families only had unscreened, young, or no offspring and so the transmission rate may be underestimated. Nevertheless, it seems likely that >50% of mosaic cases are sporadic and are not transmitted. In males, fuller analysis of germ cells will determine the level of mixed rather than strictly somatic mosaics and the level of germline mosaicism. Overall, 16/20 mosaic individuals were female, suggesting an

enrichment but this did not reach statistical significance compared to the control population (p=0.11).

Mosaicism is often considered an explanation for unilateral and severely asymmetric cases that usually have a negative family history. Indeed, we did identify six cases with asymmetric or lopsided disease. However, over the whole cohort this was not a consistent feature, and 26 fully unilateral or markedly asymmetry cases remained unresolved after these NGS-based screens. This is likely because the mosaics identified by screening blood cell DNA have broad penetrance of the mutant allele in the body's organs. Screening DNA isolated from other tissues, such as cells isolated from urine, buccal cells, hair roots, skin fibroblasts and sperm, plus methods to detect mutations at <1%, may solve these cases. Although not a significant problem in our study, the degree to which the duplicated *PKD1* gene will complicate detecting very low-level mosaicism remains to be determined.

All of the detected mosaic cases were PKD1. An enrichment for PKD1 would be expected as it is the most common ADPKD gene (~78% of cases) and a larger mutational target (~13kb coding region compared to ~3kb for *PKD2*), and mosaic PKD2 subjects may have a very mild phenotype and so not be recognized as PKD. But it does raise the question again whether *PKD1* is unusually prone to *de novo* mutations[27]. Most mutations (15/20) were deletions or insertions (~39% of germline *PKD1* mutations), 14 of which were frameshifting, including six deletions or insertions >10bp, two >250bp. It has been previously described that mosaicism of larger rearrangements is more common than for base-pair changes[28], but it is not clear if the predominance of indels here is just due to ease of detection.

The HALT PKD cohort is a typical ADPKD population where patients were hypertensive at baseline and recruited patients had either normal renal function (15-49y) or an eGFR 25-60ml/m/1.73^2 (18-64y). Notably, there was no kidney size requirement for recruitment and the finding of five different genes in this population show its diversity[9, 11, 12; 29]. All HALT PKD patients with DNA available were screened by SS[9] and unresolved and suspected mosaic cases rescreened by NGS (LR and/or tNGS). Overall, 10/831 HALT PKD families (1.2%) were shown to have ADPKD originating from a mosaic case (Table 1, Methods), with five newly resolved HALT PKD cases from the NGS analysis.

In the LR-NGS cohort, where all patients had a negative or equivocal family history and NMI from SS, seven cases were newly resolved as mosaic. Removing the patients resolved in other ways (fully penetrant *PKD1*/PKD2 mutations or other disease genes), 7/72 (9.7%) NMI families were *PKD1* mosaics. Therefore, in a typical ADPKD population, ~1% of families, and ~10% of NMI families, without a clear family history, are readily resolvable mosaics. Including very low level (<2% expected level) and high level (>50%) mosaics, the total is likely even higher, although, the representation in a population selected for rapidly progressive disease is likely to be lower[30, 31].

Methods

Study participants and clinical analysis

The participants were recruited through different ADPKD cohorts: the HALT-PKD clinical trial (n=10 positive cases: 590013, 690020, 590046, 390010, 790057, 590039, 290001, 290034, 290084, 290114)[9, 32, 33], the ADPKD Modifier Study (n=3: 870348, 870005, 870452), and the Mayo Clinic Translational PKD Center (MTPC; n=7: M484, M375, M646, M1312, M1327, M855, M174). The relevant Institutional Review Boards or ethics committees approved all studies, and participants gave informed consent. Clinical and imaging data were obtained by review of clinical and study records. Kidney function was calculated from clinical serum creatinine measurements with the Chronic Kidney Disease Epidemiology Collaboration (CKD-EPI) formula[34]. Blood samples for standard DNA isolation were collected from the probands and all available family members.

NGS of *PKD1/PKD2* LR-PCR amplicons (LR-NGS)

A total of 110 ADPKD patients were screened that had a negative/equivocal family history and were *PKD1*/*PKD2* NMI by SS. Five of the selected patients were suspected mosaic cases based on either prior SS or family data. The samples were analyzed employing a modification of the LR-PCR and NGS approach[15], which is described in detail in the Supplemental Methods and Table S3. For the bioinformatics analysis, FASTQ files were aligned to the hg19 reference genome using bwa-mem (VN:V7.10) with default options. Variant calling was performed using the GATK (VN:3.6) Haplotype Caller. Generated vcf files were prioritized for variants fulfilling the following criteria: Genotype Quality ≥20; Read Depth ≥20; Alternate Allele Frequency ≥3%; Forward/Reverse Read Balance ≥0.25; ExAc/ESP6500/1000Genome Allele Frequency ≤0.1%; Frequency Count within screened patient population <4; Exonic +/-15bp; Non-synonymous, dbNSFP Evaluation ≥ 2 as damaging (Lrt, MetaLr, PolyPhen2, Provean, SIFT). BAM files of variants of interest were reviewed and designated as possible mosaics if the alternate allele was present in 1-35% of reads.

Targeted Next-Generation Sequencing (tNGS)

Samples were run on a custom Agilent SureSelect gene panel containing the coding regions ±50bp of either 65[12] or 137 genes (Table S1). Library preparation,

sequencing, and sequence alignment was performed as described[12]. The SNP and Variation Suite (SVS, Golden Helix) was used for small nucleotide variant mining, utilizing the following filtering thresholds: variant locus read-depth (DP) ≥10 and quality (GQ) ≥20; GnomAD, MAF ≤1.0%; removal of non-coding variants >15bp from the splice site. The remaining variants were individually evaluated for pathogenicity based on: inclusion in the online ADPKD database (pkdb.pkdcure.org); or predicted loss of function, or SIFT score ≤0.10 and alignGVGD class ≥C35, and not present in an orthologous sequence; or predicted to alter splicing by Berkeley Drosophila Genome Project (BDGP) and Human Splicing Finder 3.0. BAM files of variants of interest were reviewed and designated as possible mosaics if the alternate allele was present in 1-35% of reads. Large CNVs were assessed by calculating the LOG2 ratio of actual read-depth over expected read-depth for a given locus. Variants with LOG2 ratios between 0.5 and 0.1 OR -0.2 and -0.9 were considered mosaic candidates. BAM files were reviewed to identify exact breakpoints of the CNV and the final level of mosaicism was calculated based on the change of read-depth at the 5' end of the rearrangement.

Confirmation of variants by SS, MLPA or AS-PCR

All changes were confirmed by SS for *PKD1* as previously described[14]. When family samples were available, segregation analysis of the variant of interest was performed. MLPA was performed employing the MRC Holland kits. For AS-PCR, allele specific primers were designed for mosaic variants which were not or poorly detected by SS. Either the forward or reverse primer was designed specifically to match the mutation (Table S4), with a second mismatch often introduced[35], and used to PCR amplify the mosaic variant using standard methods.

Analysis of Phenotypic Endpoints of the Mosaic Population

The most recent eGFR and htTKV available on mosaic cases and PKD1 controls (MSG 1 & 2) was employed for the regression analysis to correlate the age and phenotypic endpoints.

Acknowledgements

We thank the families and coordinators for involvement in the study and Andrew Metzger and Timothy Kline (Mayo Clinic). The study was supported by: NIDDK grant DK058816 (PCH), the Mayo Clinic Robert M. and Billie Kelley Pirnie Translational Polycystic Kidney Disease Center (DK090728; VET), an American Society of Nephrology (ASN) Foundation Ben J Lipps Fellowship (KH), ASN Kidney Research Fellowship (EC-LG), the Fulbright Association and the Foundation Monaham (EC-LG), the Zell Family Foundation and Robert M. and Billie Kelley Pirnie. The HALT-PKD studies were supported by NIDDK cooperative agreements (DK062410, DK062408, DK062402, DK082230, DK062411, and DK062401) and National Center for Research Resources General Clinical Research Centers (RR000039, RR000585, RR000054, RR000051, RR023940, RR001032) and National Center for Advancing Translational Sciences Clinical and Translational Science Awards (RR025008, TR000454, RR024150, TR00135, RR025752, TR001064, RR025780, TR001082, RR025758, TR001102, RR033179, TR000001). The ADPKD Modifier Study is supported by NIDDK grant DK079856.

Other HALT PKD and/or ADPKD Modifier Investigators are also thanked: Yu A, Winklhofer FT (Kansas Medical Center), Abebe KZ, Patterson CG (University of Pittsburgh), Schrier RW, Brosnahan GM (University of Colorado Denver), Miskulin DC (Tufts University), Braun WE (Cleveland Clinic), Czarnecki PG (Brigham and Women's Hospital), Chebib FT, Hogan MC (Mayo Clinic), Mrug M (University of Alabama at Birmingham), Pei, Y (University of Toronto), Sandford, R (University of Cambridge), Rennert H (The Rogosin Institute, NewYork), Le Meur Y (Université de Brest), Watnick, T (University of Maryland), Peter DJM (Leiden University Medical Center), Gansevoort RT (University Medical Center Groningen), Demoulin N (Université Catholique de Louvain), Devuyst O (University Hospital of Zürich).

References

1. Sampson JR, Scahill SJ, Stephenson JB*, et al.* Genetic aspects of tuberous sclerosis in the west of Scotland. *J Med Genet* 1989; **26:** 28-31.

2. Tyburczy ME, Dies KA, Glass J*, et al.* Mosaic and Intronic Mutations in TSC1/TSC2 Explain the Majority of TSC Patients with No Mutation Identified by Conventional Testing. *PLoS Genet* 2015; **11:** e1005637.

3. Rossetti S, Strmecki L, Gamble V*, et al.* Mutation analysis of the entire PKD1 gene: genetic and diagnostic implications. *Am J Hum Genet* 2001; **68:** 46-63.

4. Iliuta IA, Kalatharan V, Wang K*, et al.* Polycystic Kidney Disease without an Apparent Family History. *J Am Soc Nephrol* 2017; **28:** 2768-2776.

5. Torres VE, Harris PC, Pirson Y. Autosomal dominant polycystic kidney disease. *Lancet* 2007; **369:** 1287-1301.

6. Gabow PA, Johnson AM, Kaehny WD*, et al.* Factors affecting the progression of renal disease in autosomal-dominant polycystic kidney disease. *Kidney Int* 1992; **41:** 1311-1319.

7. Cornec-Le Gall E, Audrezet MP, Chen JM*, et al.* Type of PKD1 Mutation Influences Renal Outcome in ADPKD. *J Am Soc Nephrol* 2013; **24:** 1006-1013.

8. Irazabal MV, Rangel LJ, Bergstralh EJ*, et al.* Imaging classification of autosomal dominant polycystic kidney disease: a simple model for selecting patients for clinical trials. *J Am Soc Nephrol* 2015; **26:** 160-172.

9. Heyer CM, Sundsbak JL, Abebe KZ*, et al.* Predicted Mutation Strength of Nontruncating PKD1 Mutations Aids Genotype-Phenotype Correlations in Autosomal Dominant Polycystic Kidney Disease. *J Am Soc Nephrol* 2016; **27:** 2872-2884.

10. Clissold RL, Hamilton AJ, Hattersley AT*, et al.* HNF1B-associated renal and extra-renal disease-an expanding clinical spectrum. *Nat Rev Nephrol* 2015; **11:** 102-112.

11. Porath B, Gainullin VG, Cornec-Le Gall E*, et al.* Mutations in GANAB, Encoding the Glucosidase IIalpha Subunit, Cause Autosomal-Dominant Polycystic Kidney and Liver Disease. *Am J Hum Genet* 2016; **98:** 1193-1207.

12. Cornec-Le Gall E, Olson RJ, Besse W*, et al.* Monoallelic Mutations to DNAJB11 Cause Atypical Autosomal-Dominant Polycystic Kidney Disease. *Am J Hum Genet* 2018; **102:** 832-844.

13. Cornec-Le Gall E, Torres VE, Harris PC. Genetic Complexity of Autosomal Dominant Polycystic Kidney and Liver Diseases. *J Am Soc Nephrol* 2018; **29:** 13-23.

14. Rossetti S, Consugar MB, Chapman AB*, et al.* Comprehensive molecular diagnostics in autosomal dominant polycystic kidney disease. *J Am Soc Nephrol* 2007; **18:** 2143-2160.

15. Rossetti S, Hopp K, Sikkink RA*, et al.* Identification of gene mutations in autosomal dominant polycystic kidney disease through targeted resequencing. *J Am Soc Nephrol* 2012; **23:** 915-933.

16. Tan AY, Michaeel A, Liu G*, et al.* Molecular diagnosis of autosomal dominant polycystic kidney disease using next-generation sequencing. *J Mol Diagn* 2014; **16:** 216-228.

17. Trujillano D, Bullich G, Ossowski S*, et al.* Diagnosis of autosomal dominant polycystic kidney disease using efficient PKD1 and PKD2 targeted next-generation sequencing. *Mol Genet Genomic Med* 2014; **2:** 412-421.

18. Eisenberger T, Decker C, Hiersche M*, et al.* An efficient and comprehensive strategy for genetic diagnostics of polycystic kidney disease. *PLoS One* 2015; **10:** e0116680.

19. Braun WE, Abebe KZ, Brosnahan G*, et al.* ADPKD Progression in Patients With No Apparent Family History and No Mutation Detected by Sanger Sequencing. *Am J Kidney Dis* 2018; **71:** 294-296.

20. Connor A, Lunt PW, Dolling C*, et al.* Mosaicism in autosomal dominant polycystic kidney disease revealed by genetic testing to enable living related renal transplantation. *Am J Transplant* 2008; **8:** 232-237.

21. Consugar MB, Wong WC, Lundquist PA*, et al.* Characterization of large rearrangements in autosomal dominant polycystic kidney disease and the *PKD1/TSC2* contiguous gene syndrome. *Kidney Int* 2008; **74:** 1468-1479.

22. Reiterova J, Stekrova J, Merta M*, et al.* Autosomal dominant polycystic kidney disease in a family with mosaicism and hypomorphic allele. *BMC Nephrol* 2013; **14:** 59.

23. Tan AY, Blumenfeld J, Michaeel A*, et al.* Autosomal dominant polycystic kidney disease caused by somatic and germline mosaicism. *Clin Genet* 2015; **87:** 373-377.

24. Karczewski KJ, Francioli LC, Tiao G*, et al.* Variation across 141,456 human exomes and genomes reveals the spectrum of loss-offunction intolerance across human protein-coding genes *BioRxiv* 2019.

25. Tan AY, Zhang T, Michaeel A*, et al.* Somatic Mutations in Renal Cyst Epithelium in Autosomal Dominant Polycystic Kidney Disease. *J Am Soc Nephrol* 2018; **29:** 2139-2156.

26. Chebib FT, Jung Y, Heyer CM*, et al.* Effect of genotype on the severity and volume progression of polycystic liver disease in autosomal dominant polycystic kidney disease. *Nephrol Dial Transplant* 2016; **31:** 952-960.

27. Liu G, Myers S, Chen X*, et al.* Replication fork stalling and checkpoint activation by a PKD1 locus mirror repeat polypurine-polypyrimidine (Pu-Py) tract. *J Biol Chem* 2012; **287:** 33412-33423.

28. Kozlowski P, Roberts P, Dabora S*, et al.* Identification of 54 large deletions/duplications in TSC1 and TSC2 using MLPA, and genotype-phenotype correlations. *Hum Genet* 2007; **121:** 389-400.

29. Cornec-Le Gall E, Chebib FT, Madsen CD*, et al.* The Value of Genetic Testing in Polycystic Kidney Diseases Illustrated by a Family With PKD2 and COL4A1 Mutations. *Am J Kidney Dis* 2018; **72:** 302-308.

30. Torres VE, Chapman AB, Devuyst O*, et al.* Tolvaptan in patients with autosomal dominant polycystic kidney disease. *N Engl J Med* 2012; **367:** 2407-2418.

31. Cornec-Le Gall E, Blais J, Irazabal MV*, et al.* Can we further enrich ADPKD clinical trials for rapidly progressive patients? Application of the PROPKD score in the TEMPO trial. *Nephrol Dial Transpl* 2018; **33**: 645-652.

32. Schrier RW, Abebe KZ, Perrone RD*, et al.* Blood pressure in early autosomal dominant polycystic kidney disease. *N Engl J Med* 2014; **371:** 2255-2266.

33. Torres VE, Abebe KZ, Chapman AB*, et al.* Angiotensin blockade in late autosomal dominant polycystic kidney disease. *N Engl J Med* 2014; **371:** 2267-2276.

34. Levey AS, Stevens LA, Schmid CH*, et al.* A new equation to estimate glomerular filtration rate. *Ann Intern Med* 2009; **150:** 604-612.

35. Newton CR, Graham A, Heptinstall LE*, et al.* Analysis of any point mutation in DNA. The amplification refractory mutation system (ARMS). *Nucleic Acids Res* 1989; **17:** 2503-2516.

Table 1. Clinical presentation and genetic details of PKD1 families with mosaicism

			% reads +ve					Image Analysis								
									Kidney						Liver	
										Vol (ht)						
Pedigree	Mutation	Subject	LR-NGS	tNGS	Sex	eGFR age	HTN age (y)	Age (y)	Cystic description	RK	LK	TKV	MIC	Fig	Cystic Description	Vol (ht)
Variant transmitted																
590013	c.935_937delinsA	II-2	NS	17.3	F	63/56y	43	52	Multiple bilateral, large LK	249	639	888	1C	1D	Some small	1013
	p. Ala312fs	III-1	Offspring		M	67/29y	18	25	Multiple bilateral	326	396	722	1E	1E	Few very small	828
690020	c.12440_12443dup	II-2	9.1	NS	F	57/67y	61	61	Many large bilateral (US)	14.2^	16.6^	NA	ND		5.3cm cyst	NA
	p.Phe4149fs	III-1	Offspring		F	109/43y	41	42	Multiple bilateral	402	424	826	1C	S2A	Few small	947
870348	c.2548_2557del	II-2	NS	8.2	M	87/47y	36	47	Multiple bilateral	244	351	595	1B	1J	Few small	696
	p. Asp850fs	III-1	Offspring		M	Diagnosed at 26y but no further information available										
590046	c.8970_8972del	II-4	7.0	NS	F	91/56y	/22	53	Multiple tiny, 1 large LK	223	325	548	2A	1M	One large cyst	1529
	p.Tyr2991del	III-2	Offspring		M	127/22y	NA	19	Few bilateral	120	114	234	1B	1N	No cysts	951
		III-4	Offspring		M	NA	NA	11	Multiple bilateral (US)			NA	ND		NA	
390010	c.11654_11683del	II-2	0.1	ND	F	74/52y	/51	48	Few, 1 large RK & LK	113	144	257	1A	1Q	Few tiny	777
	p.Val3885_Ser3894del	III-1	Offspring		M	82/38y	20	35	Multiple bilateral	373	436	809	1D	1R	Multiple small	1054
Single affected individual																
790057	c.1386-34_1606+26del282bp, p.Ser463fs	II-2	NI	37.7	F	82/37	Y/29	31	Multiple bilateral	303	348	651	1C	2D	Few large	1382
590039	c.215+8043_1850-141del11.7kb, p.Leu72fs	II-4	NI	22.7, 25.5^	F	ES/55y 28/53y	Y/39	49	Multiple large bilateral	785	1073	1858	1D	2H	Severe PLD#	4228
M484	c.10922dupC, p.Arg3642fs	II-8	20.6	20.1	F	88/47y	Y/44	46	Many large bilateral	400	573	973	1C	2K	Severe PLD	3334
M375	c.11379delG, p.Thr3794fs	II-3	19.1	NS	F	113/34y	N/34	37	Multiple small	97	136	233	1A	2N	Few small	908
290001	c.4520G>A, p.Trp1507*	II-1	17.5	20.6	F	41/66y	Y/42	42	Multiple bilateral (US)			NA	ND		NA	
870005	c.844_845dupGG, p.Pro283fs	II-2	NS	14.8	F	72/54y	Y/43	49	Many large bilateral	400	431	831	1C	3C	Moderate PLD	NA
M646	c.8426C>T, p.Pro2809Leu	II-3	NS	13.4	M	44/60y	Y/<54	54	Bilateral, several large LK	206	282	487	1B	3F	None	1191
870452	c.11157-2A>G, Arg3719fs	II-2	NS	13.4	F	77/57y	Y/45	52	Multiple bilateral	527	735	1262	1C		~70 small	NA
M1312	c.5352_5353insTG, p.Asn1785*	II-2	NS	12.2	F	125/35y	N/36	36	Multiple, 1 large RK	280	256	536	1C	3K	Few tiny	536
290034	c.3685delG, p.Val1229fs	II-3	12.3	12.0	M	34/68y	Y/52	67	Bilateral renal enlargement	1506	1179	2685	1C		NA	NA
M1327	c.10373_10386del14, p.Pro3458fs	II-2	NS	9.0	M	78/48y	Y/40	46	Multiple cysts, few large	186	198	384	1B	4C	Few small	876
M855	c.74_75delGCinsT, p.Gly25fs	II-4	8.2	NS	F	76/47y	N/47	39	Multiple small RK, few LK	230	103	333	1B	4F	Multiple small	847
290084	c.1722G>T^{+}, p.Glu574Asp	II-7	6.0	7.3	F	74/53y	Y/44	50	Many large bilateral	439	359	798	1C	4I	Severe PLD	4173
M174	c.12682C>T, p.Arg4228*	II-1	7.1	3.5	F	ES/83y 16/83y	Y/64	82	Few large bilateral	512	742	1254	1B	4L	Multiple small	649
290114	c.9185_9201+7del24, Val3062fs	II-1	4.1	1.3	F	70/40y	Y/34	38	Multiple small, 3 large LK	278	164	442	1B	4O	Few small	1299

Vol (ht), height adjusted kidney or liver volume, RK, right kidney; LK, left kidney; TKV, total kidney volume; +ve, positive; y, years; F, female; M, male; HTN, hypertension (Y, yes; N, No); MIC, Mayo Imaging Class; Fig, Figure within this manuscript; NS, not screened, ND, not detected; NI, not informative; ES, ESRD, ^, kidney length; #, value before liver resection; +, predicted to disrupt splicing

Table 2. Diagnostic and family history details of PKD1 patients with mosaicism

			Proband Diagnosis			Family History				
Pedigree	Subject	Age (y)	Why	Initial Molecular	Confirmed Molecular	Father	Mother	Sibs	Children	Comments
Variant transmitted										
590013	II-2	28	Pregnancy, US	FH/ Sanger	tNGS	80y†, PC, 79y BRC	87, no PKD Dx	2, no PKD Dx	1 +ve, HALT A, III-1	Father had some cysts
690020	II-2	61	severe HTN, US	FH/Sanger	LR-NGS	>90y, no PKD Dx	~40y LTFU, no PKD Dx	2, no PKD Dx	1 +ve, HALT A, III-1 2 GD, +ve US 19y & <19y	Father reported kidney & AAA problems
870348	II-2	44	HTN, enlarged kidneys	tNGS	Sanger/AS PCR	No PKD Dx	No PKD Dx	2, no PKD Dx	1 +ve 26y, 1 untested	
590046	II-4	46	NA	FH/Sanger	LR-NGS	-ve US 78y	-ve US 76y	2 -ve US, 50, 37y, 2† other causes	2 +ve 16, 11y, 1 -ve US 10y, 1 RF untested	Brother † encephalopathy, sister MRKH, III-4, PH
390010	II-2	39	Pain, US	FH/LR-NGS	AS-PCR	76y† cardiac, no PKD Dx	80y† No PKD Dx	2, no PKD Dx, 1† accidental	1 +ve, HALT A, 1, BRC, LTFU,	
Single affected individual										
790057	II-2	30	HTN, MR	MLPA	LR-NGS	no PKD Dx	no PKD Dx, stones	3, no PKD Dx	2, NT PKD	
590039	II-4	32	Pain, imaging	MLPA	tNGS/CNV	68y† no PKD Dx	74y, no PKD Dx	4, no PKD Dx, 1 sister liver cysts	1, no PKD Dx	Distant relatives with PKD?
M484	II-8	37	Fullness, possible mass, imaging	2x NGS	Sanger	50y† EtOH, no PKD Dx	no PKD Dx	6, no PKD Dx	2, no PKD Dx	
M375	II-3	26	CT, Pain	Sanger	LR-NGS	†MI, no PKD Dx	2 liver cysts	3, no PKD Dx	None	
290001	II-1	42	US	2xNGS	Sanger	No PKD Dx	no PKD Dx	None	2 -ve US, 20y, 14y, 1 untested	
870005	II-2	43	Pain, imaging	tNGS	Sanger	†melanoma, no PKD Dx	no PKD Dx	1, no PKD Dx	3, untested	
M646	II-3	53	HTN, US	tNGS	Sanger	no PKD Dx	no PKD Dx	4, no PKD Dx	1, no PKD Dx	
870452	II-2	45	HTN, flank pain, imaging	tNGS	Sanger	no PKD Dx, 76y	no PKD Dx, 75y	1, no PKD Dx, 57y	1 -ve US, 2 untested	Grandfather ESRD 75y
M1312	II-2	25	Pregnancy US	tNGS	AS-PCR	-ve US	-ve US	1, -ve US	4 untested	6mm kidney stone
290034	II-3	56	Hematuria, imaging	2x NGS	Sanger	77y†, no PKD Dx	no PKD Dx	2, no PKD Dx	1 no PKD, 1 untested	
M1327	II-2	46	Cyst hemorrhage	tNGS	Sanger	-ve US, 70s, MND	-ve US, 70s, MND	2, no PKD Dx	3 untested	
M855	II-4	38	Pain, US	Sanger	LR-NGS	-ve US, 72y	-ve US, 68y	3, no PKD Dx	3 no PKD Dx	
290084	II-7	44	HTN, CT	2x NGS	AS-PCR	no PKD Dx, 83y	no PKD Dx, 77y	6, no PKD Dx	2 no PKD Dx	
M174	II-1	64	Fullness, CT	2x NGS	Sanger	78y†, no PKD Dx	94y†, no PKD Dx	2, no PKD Dx	1 adopted	
290114	II-1	35	Stones, HTN, MR	2x NGS	Sanger	no PKD Dx	no PKD Dx	None	3 no PKD Dx	

US, ultrasound; HTN, hypertension; FH, family history; 2x NGS, both the LR- and tNGS methods; PC, pancreatic cancer; †, died; BRC, bilateral renal cysts; EtOH, alcoholic; MI, myocardial infarction; MND, mutation not detected; LTFU, lost to follow up; RF, reflux; AAA, abdominal aortic aneurysm, MRKH, Mayer Rokitansky, Küster Hauser syndrome; PH, prenatal hydrocephalous; y, years; GD, granddaughter; CT, computer tomography; MR, magnetic resonance; Dx, diagnosis

Figure Legends

Figure 1. Pedigree, imaging and sequencing data of mosaic families segregating the mutation to the next generation. (**A**) Pedigree 590013 showing ADPKD in II-2 and III-1, with I-1 found to have a few, likely simple, cysts at 79y. (**B**) SS showing the indel (red line) and reduced peak height of the frameshifted sequence (red) in II-2 compared to III-1. (**C**) tNGS showing the CCG deletion and T insertion in a reduced number of reads in II-2 compared to III-1. (**D**) MRI of II-2 at 47y showing asymmetric disease with just a few large cysts in the left kidney compared to a more even distribution in III-1 (**E**). (**F**) Pedigree 690020 with ADPKD in three generations. (**G**) SS of II-2 showing the frameshifted sequence following the 4bp duplication at a low level, reflecting mosaicism. (**H**) Pedigree of family 870348 with ADPKD in II-2 and III-1. (**I**) SS of II-2 (reverse strand) showing frameshifted sequence due to a 10bp deletion at a very low level, which is confirmed by AS-PCR (Figure S2B). (**J**) MRI showing robust PKD in II-2. (**K**) Pedigree 590046 showing the mosaic case (II-4) with two affected children (III-2 and III-4). (**L**) The inframe codon deletion is seen at only a low level in II-4 compared to III-2. (**M**) MRI of II-4 showing very mild kidney and liver cystic disease. (**N**) Contrast (C) enhanced CT of III-2 at 19y showing a few kidney cysts. (**O**) Pedigree 390010 shows ADPKD in the II-2 and III-1. (**P**) SS of the AS-PCR from a normal individual (N), the son (III-1) and the mosaic mother (II-2) shows the 30bp deletion in the son, but due to the low-level mosaicism, the AS-PCR is not completely specific in II-2, hence the doublet sequence. (**Q**) CT of II-2 shows just a couple of cysts, in contrast to the typical PKD shown by MRI in III-1 (**R**). Pedigree: red shaded, mosaic; gray, equivocal or unknown; white, ADPKD negative.

Figure 2. Pedigree, imaging and sequencing data of mosaic families not segregating the mutation (I). (**A**) Pedigree 790057 showing the mosaic mother (II-2) and her untested offspring. (**B**) Screening by MLPA found a possible mosaic deletion of ex7 that was confirmed by log2 copy number variant (CNV) analysis of the LR-NGS (**C**). (**D**) MRI of II-2 shows typical ADPKD at 31y. (**E**) Pedigree 590039 shows the mosaic subject (II-4) as the only affected. (**F**) A suspected mosaic *PKD1* deletion was detected by MLPA and confirmed by log2 CNV analysis (Figure **S2D**). (**G**) Amplification and SS (Figure **S2E**) of a specific breakpoint fragment defined the deletion. (**H**) MRI of II-4 shows

significant kidney disease at 49y (prior to ESRD) and severe PLD (after partial liver resection). (**I**) Pedigree M484 showing two untested daughters of the mosaic case (II-8). (**J**) Sanger confirmation of the mosaic single nucleotide duplication in II-8. (**K**) Non-contrast (NC) enhanced CT of II-8 at 46y shows significant PKD and severe PLD. (**L**) Pedigree M375 shows just one affected subject (II-3). (**M**) Sanger sequence shows II-3 is mosaic for a single nucleotide deletion. (**N**) CT of II-3 at 37y shows very mild kidney disease. (**O**) Pedigree 290001 shows the mosaic subject (II-1) and three children without PKD or untested. (**P**) Sanger sequence of II-1 confirms mosaicism of a nonsense mutation. Pedigree: red shaded, mosaic; gray, equivocal or unknown; white, ADPKD negative.

Figure 3. Pedigree, imaging and sequencing data of mosaic families not segregating the mutation (II). (**A**) Pedigree 870005 where the mosaic subject (II-2) has three untested children. (**B**) SS confirmation in II-2 of mosaicism of the GG duplication (reverse strand shown). (**C**) MRI of II-2 at 49y shows multiple large cysts. (**D**) Pedigree M646 where the mosaic proband (II-3) has an untested son. (**E**) SS confirms mosaicism for a previously described missense substitution in II-3. (**F**) CT imaging of II-3 at 54y shows bilateral disease with large cysts in the left kidney. (**G**) Pedigree 870452 showing three offspring of the mosaic case II-2. (**H**) SS of II-2 confirms mosaicism for a typical splicing mutation. (**I**) Pedigree M1312 shows mosaicism in II-2 with four untested children. (**J**) AS-PCR shows a specific fragment just in II-2 but not the normal (N) control, that was confirmed to have the TG insertion by SS of the product (Figure **S2F**). (**K**) CT of II-2 at 36y shows bilateral cysts with several large cysts in the right kidney. (**L**) Pedigree 290034 indicates mosaicism in II-3 and two children either negative or untested. (**M**) Sanger sequence of II-3 confirms mosaicism of a G deletion. Pedigree: red shaded, mosaic; gray, equivocal or unknown; white, ADPKD negative.

Figure 4. Pedigree, imaging and sequencing data of mosaic families not segregating the mutation (III). (**A**) Pedigree M1327 shows the mosaic proband (II-2) has untested twin girls and a son. (**B**) SS of II-2 confirms mosaicism for a 14bp deletion. (**C**) Just a few bilateral cysts are detected in II-2 by MRI at 46y. (**D**) The mosaic proband in M855 (II-4) has 3 untested children. (**E**) SS of II-4 confirms mosaicism of a

deletion/insertion mutation. (**F**) CT of II-4 at 39y show just a few small cysts in the kidney and liver. (**G**) Pedigree 290084 shows two offspring of the mosaic subject (II-7) either negative for PKD or untested. (**H**) AS-PCR shows the mutant allele just in II-7 but not a control (N), and sequencing confirms the substitution (Figure **S2G**). (**I**) MRI of II-7 show moderate kidney disease and severe PLD. (**J**) The mosaic proband (II-1) in M174 is the only affected member. (**K**) AS-PCR shows that II-1 has the p.Arg4228* mutation that is also found in a positive control (P) but not an individual without this change (N), and SS shows the substitution at a very low level (Figure **S2H**). (**L**) CT of II-1 at 82y, shortly before ESRD, shows a few large cysts in both kidneys. (**M**) Pedigree 290114 shows the mosaic individual (II-1) has three untested children. (**N**) SS of II-1 shows mosaicism for a 24bp, splice site spanning, deletion. (**O**) II-1 has mild cystic disease with a few moderately sized cysts. Pedigree: red shaded, mosaic; gray, equivocal or unknown; white, ADPKD negative.

Figure 5. Regression comparison of eGFR and htTKV in mosaic subjects compared to PKD1 controls. The control populations (blue) are PKD1 patients with truncating (MSG1) or strongly predicted non-truncating changes (MSG2)[9] from a MTPC cohort without known mosaicism; n=550 for eGFR and 403 for htTKV. The mosaic population is indicated in red and the percentage level of the mosaic allele compared to a fully penetrant allele is listed for each case. (**A**) The renal function analysis shows that the mosaic population (red) has a significantly higher eGFR than the controls (blue). (**B**) Analysis of renal structure shows that the mosaic population has a significantly lower htTKV than the controls. The htTKV is plotted on a log2 scale. No correlation was observed between the level of mosaicism and disease severity (eGFR or htTKV).

Fig 1

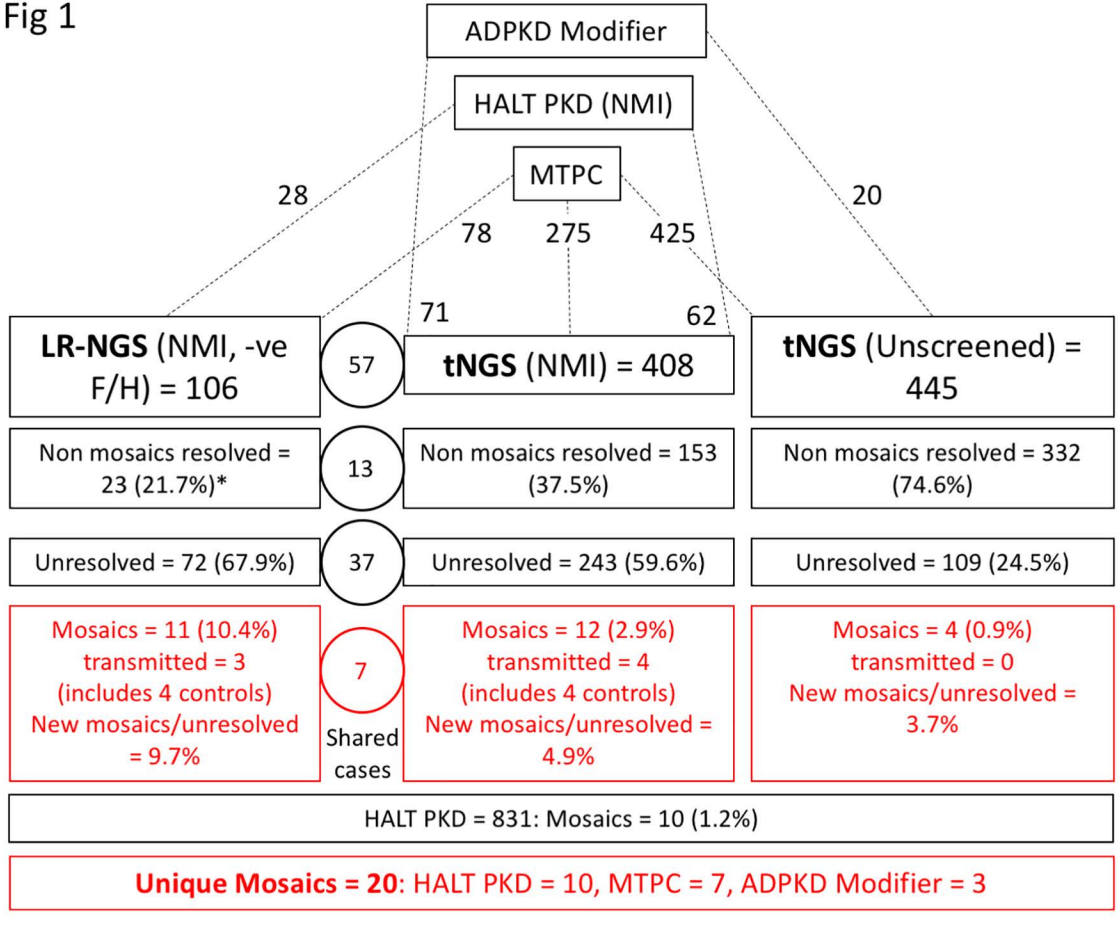
ADPKD Modifier
HALT PKD (NMI)
MTPC
28
78
275
425
20
71
62
LR-NGS (NMI, -ve F/H) = 106
57
tNGS (NMI) = 408
tNGS (Unscreened) = 445
Non mosaics resolved = 23 (21.7%)*
13
Non mosaics resolved = 153 (37.5%)
Non mosaics resolved = 332 (74.6%)
Unresolved = 72 (67.9%)
37
Unresolved = 243 (59.6%)
Unresolved = 109 (24.5%)
Mosaics = 11 (10.4%)
transmitted = 3
(includes 4 controls)
New mosaics/unresolved = 9.7%
7
Shared cases
Mosaics = 12 (2.9%)
transmitted = 4
(includes 4 controls)
New mosaics/unresolved = 4.9%
Mosaics = 4 (0.9%)
transmitted = 0
New mosaics/unresolved = 3.7%
HALT PKD = 831: Mosaics = 10 (1.2%)
Unique Mosaics = 20: HALT PKD = 10, MTPC = 7, ADPKD Modifier = 3

Fig 2

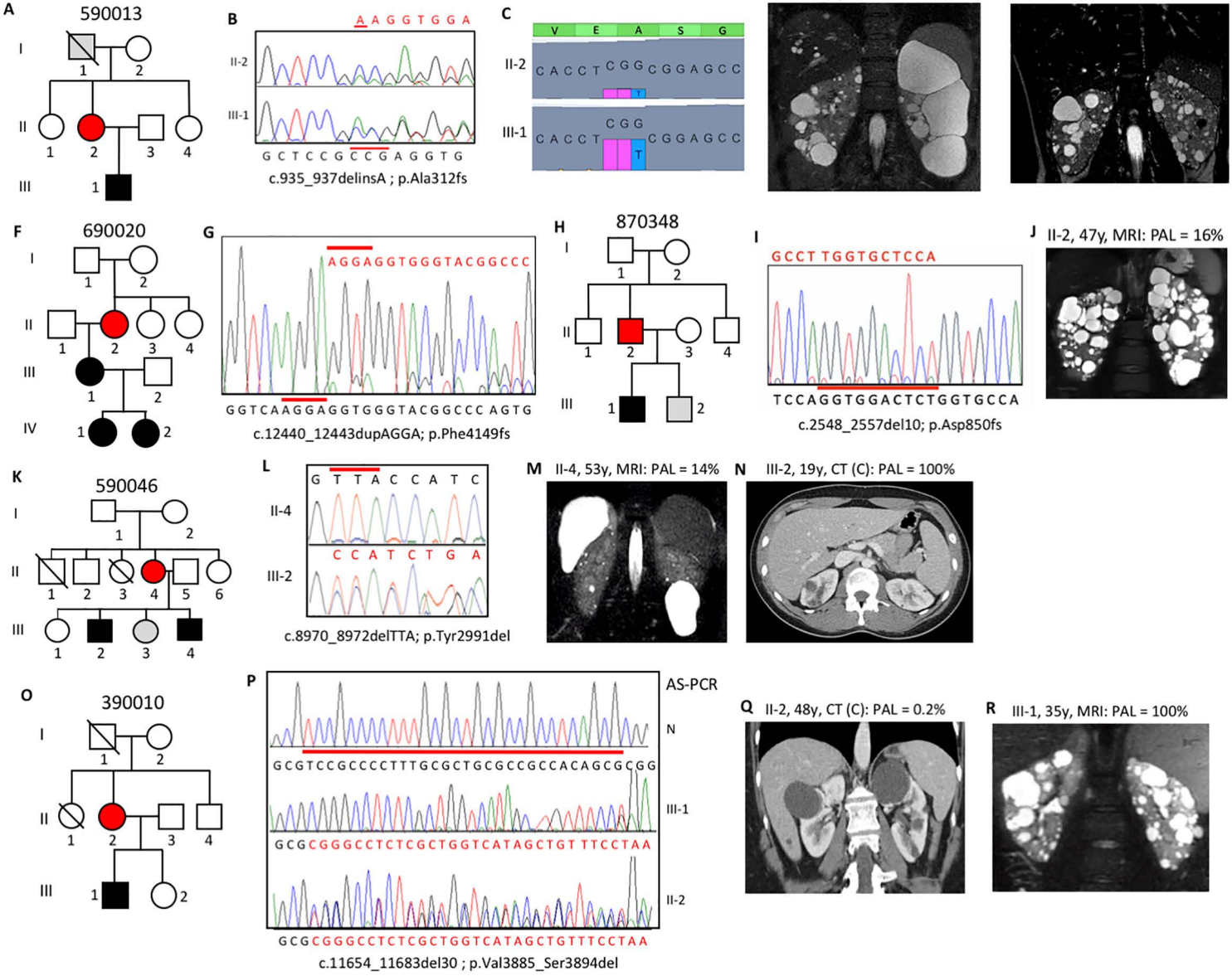
A
590013
I
1
2
II
1
2
3
4
III
1
B
A A G G T G G A
II-2
III-1
G C T C C G C C G A G G T G
c.935_937delinsA ; p.Ala312fs
C
V E A S G
II-2
C A C C T C G G C G G A G C C
T
III-1
C G G
C A C C T C G G A G C C
T
D
II-2, 47y, MRI: PAL = 35%
E
III-1, 20y, MRI: PAL =100%
F
690020
I
1
2
II
1
2
3
4
III
1
2
IV
1
2
G
A G G A G G T G G G T A C G G C C C
G G T C A A G G A G G T G G G T A C G G C C C A G T G
c.12440_12443dupAGGA; p.Phe4149fs
H
870348
I
1
2
II
1
2
3
4
III
1
2
I
G C C T T G G T G C T C C A
T C C A G G T G G A C T C T G G T G C C A
c.2548_2557del10; p.Asp850fs
J
II-2, 47y, MRI: PAL = 16%
K
590046
I
1
2
II
1
2
3
4
5
6
III
1
2
3
4
L
G T T A C C A T C
II-4
C C A T C T G A
III-2
c.8970_8972delTTA; p.Tyr2991del
M
II-4, 53y, MRI: PAL = 14%
N
III-2, 19y, CT (C): PAL = 100%
O
390010
I
1
2
II
1
2
3
4
III
1
2
P
AS-PCR
N
G C G T C C G C C C C T T T G C G C T G C G C C G C C A C A G C G C G G
III-1
G C G C G G G C C T C T C G C T G G T C A T A G C T G T T T C C T A A
II-2
G C G C G G G C C T C T C G C T G G T C A T A G C T G T T T C C T A A
c.11654_11683del30 ; p.Val3885_Ser3894del
Q
II-2, 48y, CT (C): PAL = 0.2%
R
III-1, 35y, MRI: PAL = 100%

Fig 3

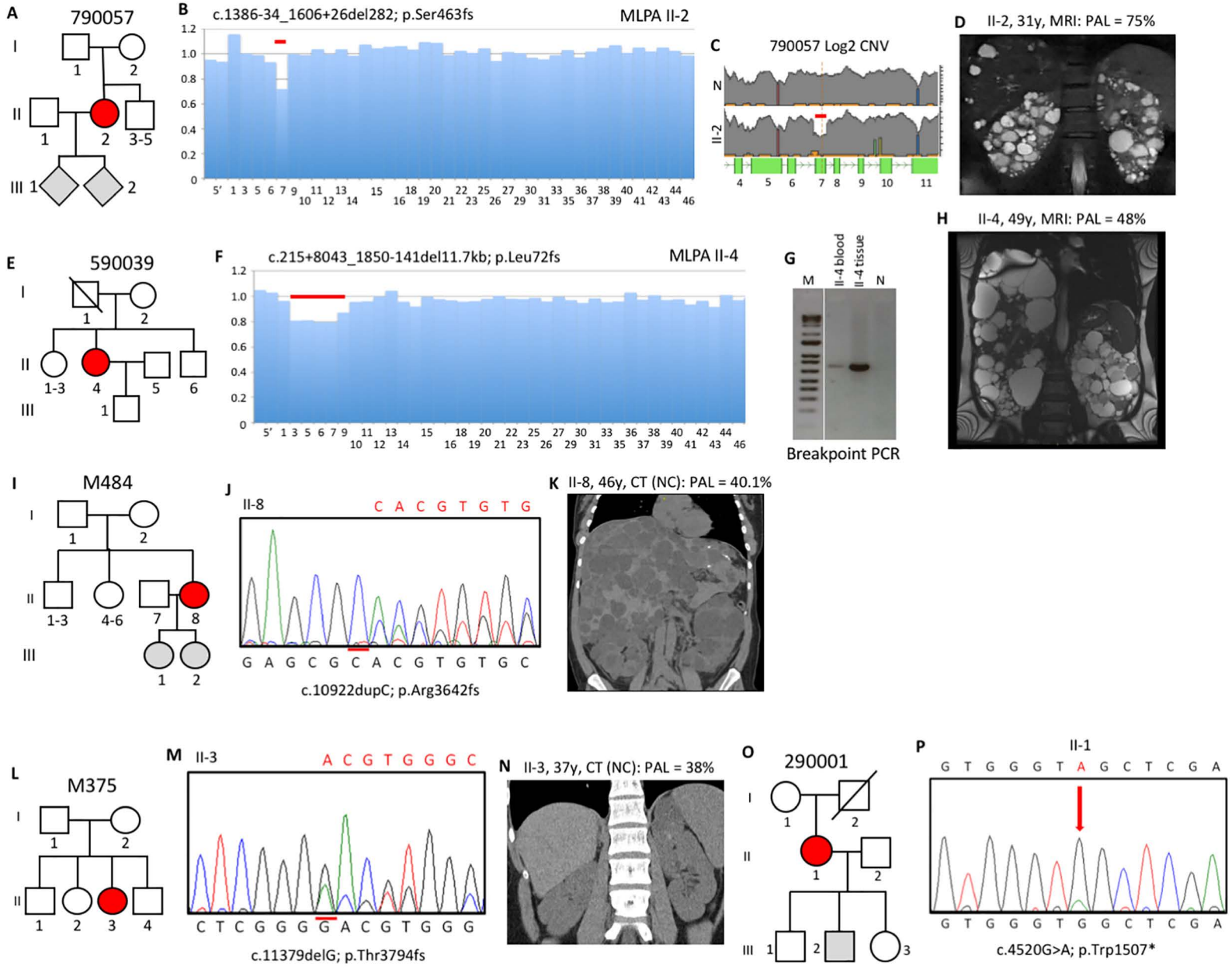
A
790057
B
c.1386-34_1606+26del282; p.Ser463fs
MLPA II-2
C
790057 Log2 CNV
N
II-2
D
II-2, 31y, MRI: PAL = 75%
E
590039
F
c.215+8043_1850-141del11.7kb; p.Leu72fs
MLPA II-4
G
M
II-4 blood
II-4 tissue
N
Breakpoint PCR
H
II-4, 49y, MRI: PAL = 48%
I
M484
J
II-8
C A C G T G T G
G A G C G C A C G T G T G C
c.10922dupC; p.Arg3642fs
K
II-8, 46y, CT (NC): PAL = 40.1%
L
M375
M
II-3
A C G T G G G C
C T C G G G G A C G T G G G
c.11379delG; p.Thr3794fs
N
II-3, 37y, CT (NC): PAL = 38%
O
290001
P
II-1
G T G G G T A G C T C G A
G T G G G T G G C T C G A
c.4520G>A; p.Trp1507*

Fig 4

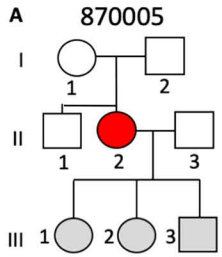
A
870005
I
1
2
II
1
2
3
III
1
2
3

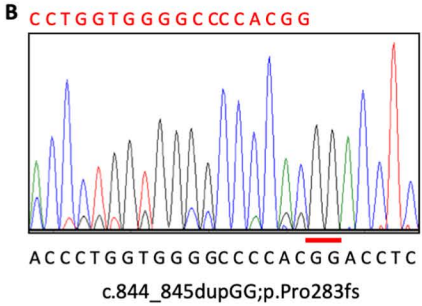
B
C C T G G T G G G G C C C C A C G G
A C C C T G G T G G G G C C C C A C G G A C C T C
c.844_845dupGG;p.Pro283fs

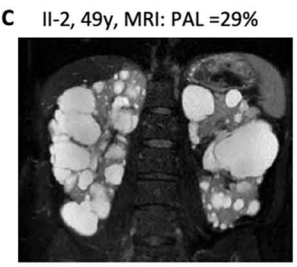
C
II-2, 49y, MRI: PAL =29%

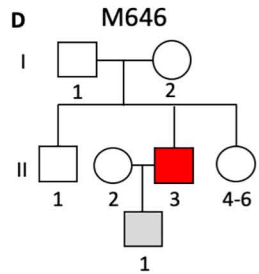
D
M646
I
1
2
II
1
2
3
4-6
1

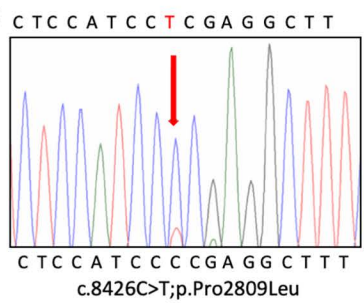
E
C T C C A T C C T C G A G G C T T
C T C C A T C C C C G A G G C T T T
c.8426C>T;p.Pro2809Leu

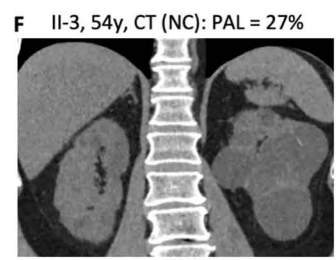
F
II-3, 54y, CT (NC): PAL = 27%

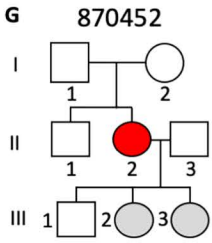
G
870452
I
1
2
II
1
2
3
III
1
2
3

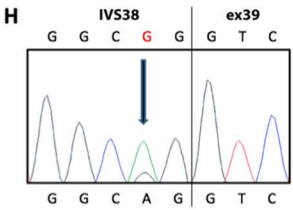
H
IVS38
ex39
G G C G G G T C
G G C A G G T C
c.11157-2A>G;p.Arg3719fs

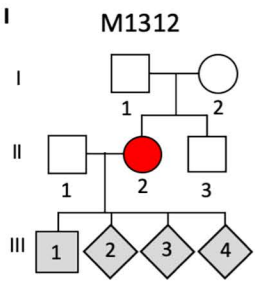
I
M1312
I
1
2
II
1
2
3
III
1
2
3
4

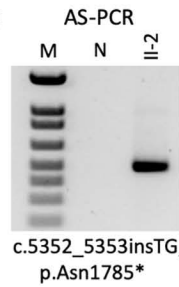
J
AS-PCR
M
N
II-2
c.5352_5353insTG,
p.Asn1785*

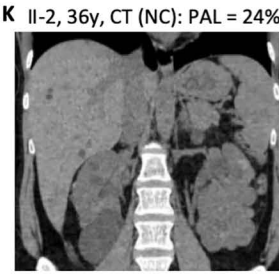
K
II-2, 36y, CT (NC): PAL = 24%

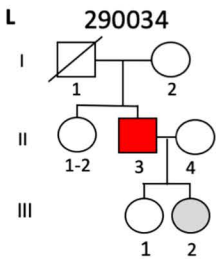
L
290034
I
1
2
II
1-2
3
4
III
1
2

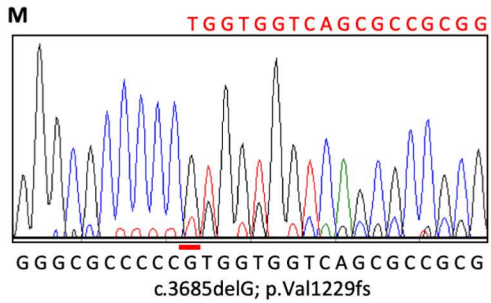
M
T G G T G G T C A G C G C C G C G G
G G G C G C C C C C G T G G T G G T C A G C G C C G C G
c.3685delG; p.Val1229fs

Fig 5

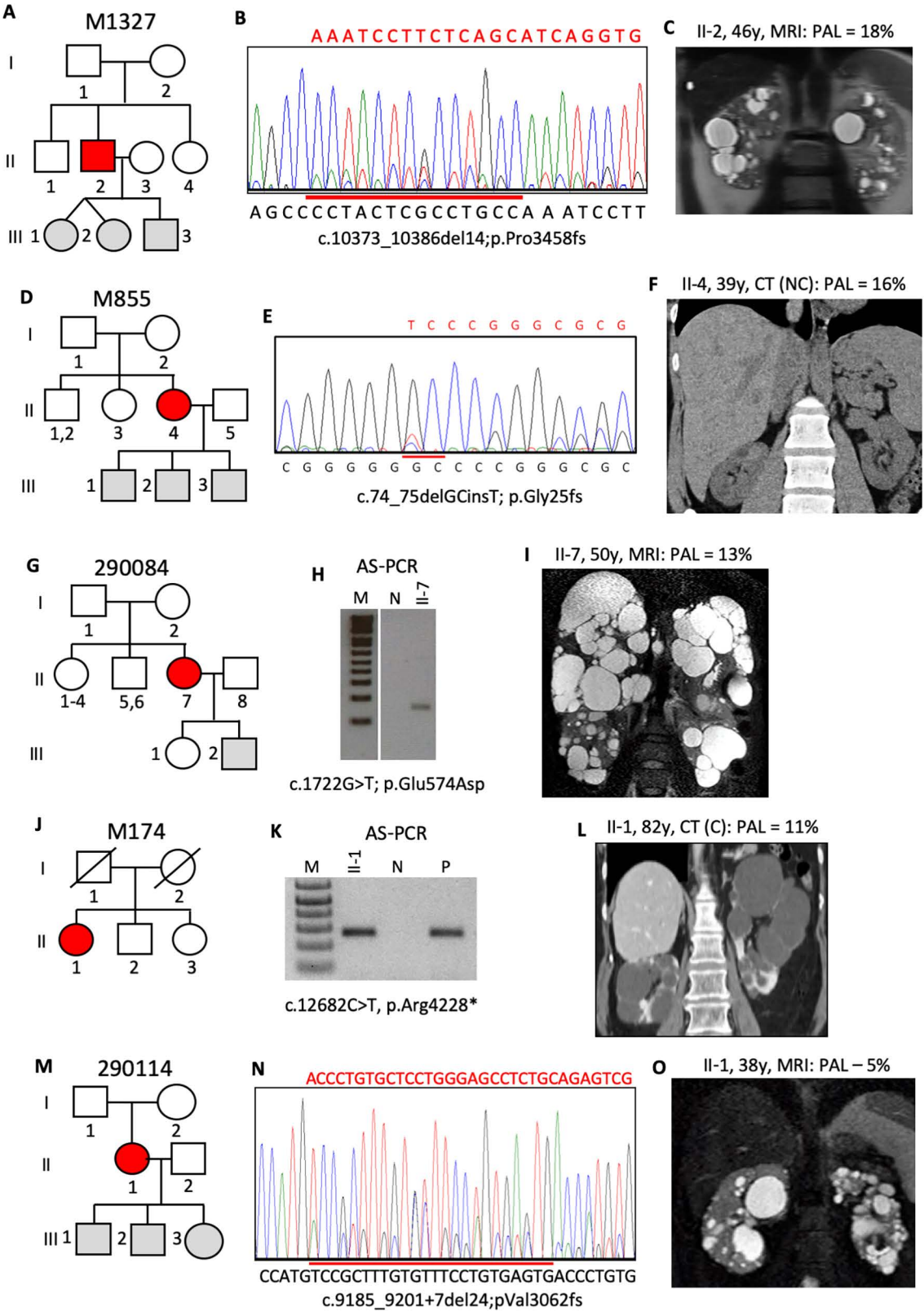
A
M1327
I
1
2
II
1
2
3
4
III 1
2
3
B
AAATCCTTCTCAGCATCAGGTG
AGCCCCTACTCGCCTGCCA A ATCCTT
c.10373_10386del14;p.Pro3458fs
C
II-2, 46y, MRI: PAL = 18%
D
M855
I
1
2
II
1,2
3
4
5
III
1
2
3
E
T C C C G G G C G C G
C G G G G G G C C C C G G G C G C
c.74_75delGCinsT; p.Gly25fs
F
II-4, 39y, CT (NC): PAL = 16%
G
290084
I
1
2
II
1-4
5,6
7
8
III
1
2
H
AS-PCR
M
N
II-7
c.1722G>T; p.Glu574Asp
I
II-7, 50y, MRI: PAL = 13%
J
M174
I
1
2
II
1
2
3
K
AS-PCR
M
II-1
N
P
c.12682C>T, p.Arg4228*
L
II-1, 82y, CT (C): PAL = 11%
M
290114
I
1
2
II
1
2
III 1
2
3
N
ACCCTGTGCTCCTGGGAGCCTCTGCAGAGTCG
CCATGTCCGCTTTGTGTTTCCTGTGAGTGACCCTGTG
c.9185_9201+7del24;pVal3062fs
O
II-1, 38y, MRI: PAL – 5%

Fig 6

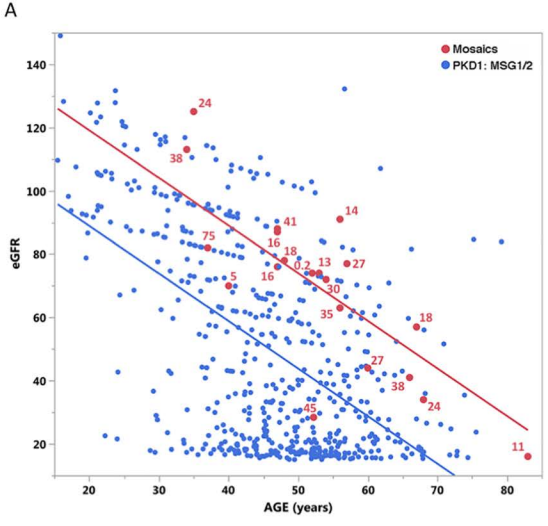
A
Mosaics
PKD1: MSG1/2
eGFR
AGE (years)
140
120
100
80
60
40
20
20
30
40
50
60
70
80
24
38
41
14
75
16
18
0.2
13
27
5
16
30
35
18
27
38
24
45
11

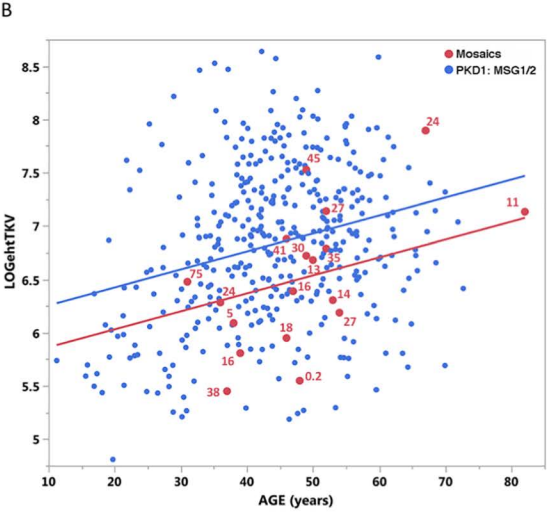
B
Mosaics
PKD1: MSG1/2
LOGehtTKV
AGE (years)
8.5
8
7.5
7
6.5
6
5.5
5
10
20
30
40
50
60
70
80
24
45
27
11
41
30
35
13
75
24
16
14
5
27
18
16
0.2
38